

The ratio of the numbers of hyperfragments projected in the forward and backward directions in this experiment can also be understood in terms of the above model. The hyperfragments of short ranges arising from Λ^0 trapping in the residual nuclei would be expected to be markedly influenced by the direction of flight of the K^- mesons. The hyperfragments of longer range would be expected to have a smaller forward to backward ratio if they were mainly evaporated from a slowly moving nucleus.

A similar model may be applied to the interpretation of hyperfragment production by K^- mesons at rest. In this case the momenta of the residual hypernuclei would be expected to be smaller so that fewer of them would have sufficient momentum to form an observable track in the emulsion. This is consistent with the estimate of D. H. Davis *et al.* of the formation of cryptofragments (i.e., hyperfragments which do not produce recognizable tracks) in as many as 30% of the interactions of stopping K^- mesons with emulsion nuclei.¹⁸

¹⁸ D. H. Davis, M. Csejthey-Barth, J. Sacton, B. D. Jones,

ACKNOWLEDGMENTS

We wish to thank Professor E. J. Lofgren and the Bevatron team for making the facilities of the Bevatron available to us and Dr. D. Keefe for carrying out the exposure. We are much indebted to Dr. E. Brunninx, Dr. D. Evans, Dr. P. H. Fowler, Dr. W. Gibson, Dr. W. O. Lock, Dr. G. Rudstam, and Dr. S. St. Lorant for many helpful discussions.

Acknowledgment is also made to the Department of Scientific and Industrial Research for a special development grant to University College London and research scholarships to B. D. Jones and J. Zakrzewski, and to the Indian Ministry of Education and the University of Mysore for an overseas scholarship to B. Sanjeevaiah.

B. Sanjeevaiah, and J. Zakrzewski, *Nuovo cimento* **22**, 275 (1961); see, however, B. Cester, G. Ciochetti, A. Debenedetti, A. Marzari Chiesa, R. Rinaudo, C. Deney, K. Gottstein, and W. Püschel *Nuovo cimento* **22**, 1069 (1961); and A. Filipkowski, E. Marquit, E. Skrzypszak, and A. Wroblewski (to be published).

Reaction $p+p \rightarrow \pi^+ + p + n$ at 405 MeV*

R. L. McILWAIN,[†] K. J. DEAHL,[‡] M. DERRICK,[§] J. G. FETKOVICH, AND T. H. FIELDS||

Department of Physics, Carnegie Institute of Technology, Pittsburgh, Pennsylvania

(Received February 20, 1962)

The azimuthal asymmetry of pion production in the reaction $p+p \rightarrow \pi^+ + p + n$ was measured using the 53% polarized 405-MeV proton beam from the Carnegie Institute of Technology's synchrocyclotron. Pions produced in a liquid hydrogen target were successively detected on the left and on the right by means of their stopping and subsequent $\pi\mu e$ decay in a 6-in. propane bubble chamber. Elastically scattered protons were used to monitor the incident beam intensity. The pions which stopped in the chamber had an average c.m. momentum of $0.52 \mu c$ and c.m. production angles between 80 and 105°. The observed pion asymmetry is $|\epsilon| = (20 \pm 6.5)\%$, in the same direction as the previously observed asymmetry for the $(p p, \pi^+ d)$ reaction. The similarity between the observed pion asymmetry and that for the $(p p, \pi^+ d)$ reaction suggests that their reaction amplitudes are similar, and thus that 3S rather than P states are predominant for the final-state nucleons in the $(p p, \pi^+ p n)$ reaction at this energy. The estimated total cross section (0.63 ± 0.06 mb) is in good agreement with the calculation of Mandelstam.

INTRODUCTION

THE production of single positive pions in proton-proton collisions can proceed through either of the following reactions:

$$p + p \rightarrow \pi^+ + d, \quad (1)$$

$$p + p \rightarrow \pi^+ + p + n. \quad (2)$$

Numerous measurements of the total cross section

* This work was supported in part by the U. S. Atomic Energy Commission.

[†] Now at Princeton University, Princeton, New Jersey. A thesis based on this work has been submitted by R. L. McIlwain in partial fulfillment of the requirements for the degree of Doctor of Philosophy at the Carnegie Institute of Technology.

[‡] Now at I.B.M., Silver Springs, Maryland.

[§] Now at Oxford University.

|| Now at Northwestern University, Evanston, Illinois.

and angular distribution for these reactions (using unpolarized proton beams) have been made. Also, the azimuthal asymmetry of reaction (1) with a polarized incident beam has been measured at several energies. For the threshold region ($E_p \lesssim 450$ Mev), the experimental results have been interpreted in terms of a phenomenological theory, allowing the identification of the principal angular momentum channels (pion with $l=0$ or 1, and final-state nucleons in a relative 3S_1 state) and forming a picture which seems consistent with the experimental results in that energy region.¹ The threshold theory neglects the final-state pion-

¹ M. Gell-Mann and K. M. Watson, *Ann. Rev. Nuclear Sci.* **4**, 219 (1954).

nucleon interaction and treats the final-state nucleon-nucleon interaction with a zero-range approximation.

For energies above the threshold region it is important to take into account the final-state pion-nucleon interaction as well as the possibility that the final-state nucleons are in a relative P state. Mandelstam has treated both the pion-nucleon and nucleon-nucleon final interactions explicitly, thereby extending the theory to region of higher energy.² He obtained a three-parameter theory which can be fitted to experimental data quite well up to 900 MeV. Figures 1 and 2 show total cross-section data as well as the appropriate results of Mandelstam's calculations.

In this experiment, the azimuthal asymmetry of the positive pions produced in reaction (2) was measured, using a polarized proton beam. This measurement was made in order to provide another measure of the extent to which 405 MeV is still within the threshold region; that is, in the threshold region the dynamics of the two reactions are assumed to be essentially identical except for the n - p final-state interaction leading to either a bound or unbound 3S_1 state. If the assumptions of the threshold theory were invalid, this essential similarity between the two reactions should not hold.

Figure 3 shows measured values for the azimuthal asymmetry of reaction (1). For brevity, we shall not

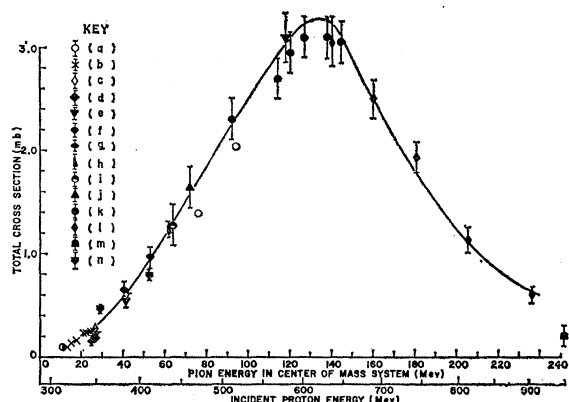


FIG. 1. Total cross section for the reaction $p + p \rightarrow \pi^+ + d$. The reference points listed are as follows: (a) H. L. Stadler, Phys. Rev. **96**, 496 (1954); (b) F. S. Crawford and M. L. Stevenson, Phys. Rev. **97**, 1305 (1955); (c) D. L. Clark, A. Roberts, and R. Wilson, Phys. Rev. **83**, 649 (1951); (d) W. F. Cartwright, C. Richman, M. N. Whitehead, and H. A. Wilcox, Phys. Rev. **91**, 677 (1953); (e) J. R. Holt, J. C. Kluyver, and J. A. Moore, Proc. Phys. Soc. (London) **A71**, 781 (1957); (f) R. Durbin, H. Loar, and J. Steinberger, Phys. Rev. **84**, 581 (1951); (g) M. N. Whitehead and C. Richman, Phys. Rev. **83**, 855 (1951); (h) T. H. Fields, J. G. Fox, J. A. Kane, R. A. Stallwood, and R. B. Sutton, Phys. Rev. **109**, 1704 (1958); (i) C. E. Cohn, Phys. Rev. **105**, 1582 (1957); (j) M. G. Meshcheryakov, B. S. Neganov, N. P. Bogachev, and V. M. Siderov, Doklady Akad. Nauk, SSSR, **100**, 673 (1955); (k) M. G. Meshcheryakov and B. S. Neganov, Doklady Akad. Nauk, SSSR, **100**, 677 (1955); (l) B. S. Neganov and L. B. Parfenov, Soviet Phys.—JETP **7**, 528 (1958); (m) A. P. Batson, B. B. Culwick, and L. Riddiford, Proc. Roy. Soc. (London) **A251**, 218 (1959); (n) A. M. Sachs, H. Winick, and B. A. Wooten, Phys. Rev. **109**, 1733 (1958).

² S. Mandelstam, Proc. Roy. Soc. (London) **A244**, 491 (1958).

include a quantitative discussion of the threshold theory here. See references 1 and 2. We shall use the notation of reference 1.

EXPERIMENTAL METHOD

The circulating proton beam of the Carnegie synchrocyclotron was scattered from an internal carbon target through an angle of $(10 \pm 1)^\circ$. The scattered beam had an energy of (415 ± 10) MeV, a polarization of 0.53 ± 0.03 , an angular spread of $\pm 0.5^\circ$, and an intensity of about 4×10^4 /pulse. A differential range curve of the beam is shown in Fig. 4.

In the experimental area the beam traversed a liquid hydrogen target 6 in. wide and 18 in. in the beam direction. The average energy of the beam at the center of the target was 405 MeV. The experimental arrange-

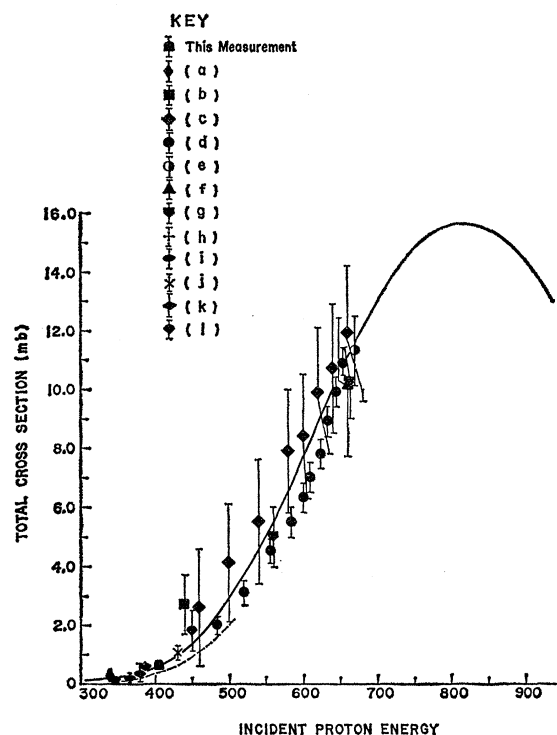


FIG. 2. Total cross section for the reaction $p + p \rightarrow \pi^+ + p + n$. The reference points listed are as follows: (a) J. R. Holt, J. C. Kluyver, and J. A. Moore, Proc. Phys. Soc. (London) **A71**, 781 (1957); (b) A. H. Rosenfeld, Phys. Rev. **96**, 130, 139 (1954); (c) V. P. Dzelepov, V. I. Moskalev, and S. V. Medved, Doklady Akad. Nauk, SSSR, **104**, 380 (1955); (d) B. S. Neganov and O. V. Savchenko, Soviet Phys.—JETP **5**, 1033 (1957); (e) A. G. Meshkovskii, Ia. Ia. Shalamov, and V. A. Shebanov, Soviet Phys.—JETP **8**, 46 (1959); (f) V. M. Siderov, Soviet Phys.—JETP **4**, 22 (1957); (g) M. G. Meshcheryakov, V. P. Zrellov, B. S. Neganov, I. K. Vzorov, and A. F. Shabudin, Soviet Phys.—JETP **4**, 60 (1957); (h) A. P. Batson, B. B. Culwick, and L. Riddiford, Proc. Royal Soc. (London) **A251**, 218 (1959); (i) M. Block, S. Passman, and W. W. Havens, Jr., Phys. Rev. **88**, 1239 and 1247 (1952); (j) T. H. Fields, J. G. Fox, J. A. Kane, R. A. Stallwood, and R. B. Sutton, Phys. Rev. **109**, 1713 (1958); (k) M. H. Alston, A. V. Crewe, W. H. Evans, and G. von Gierke, Proc. Phys. Soc. (London) **A69**, 691 (1956); (l) L. G. Pondrom, Phys. Rev. **114**, 1623 (1959).

ment is shown in Fig. 5. Pions produced in the laboratory angular region between 30° and 63° and with laboratory energy between 30 and 55 MeV came to rest within a $2 \times 3 \times 6$ -in. propane (C_3H_8) bubble chamber. Half of the pictures were taken with the chamber on the right side of the beam and the rest were taken on the left. The pions were detected by observing their characteristic $\pi^+ \rightarrow \mu^+ \rightarrow e^+$ decay. The beam intensity was monitored by counting the number of elastically scattered protons in the bubble chamber pictures and using the known p - p elastic scattering cross section to calculate the incident flux.

A dummy target was constructed as an aid in estimating the background from the target ends. This consisted of two $\frac{1}{4}$ -in. thick copper plates mounted at the normal position of the target ends. Thus it was possible to obtain an accurate estimate of the angular distribution of the tracks emanating from the ends of the hydrogen container.

A total of 52 000 pictures was taken, including 400 using the copper dummy target, and 500 with the hydrogen target empty.

The pictures were first scanned for $\pi-\mu-e$ decays in the propane. All doubtful events were reported. Each view of the stereo pair was scanned independently by the same scanner. All events reported in the initial scan were examined carefully to determine if they were $\pi-\mu-e$ decays. Only four of approximately 1500 reported events could not be resolved, and they were discarded. Each scanner scanned successively 100 ft rolls from alternate sides of the beam. Approximately

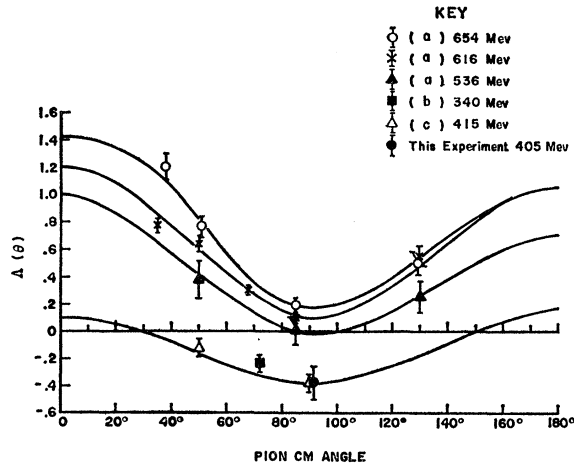


FIG. 3. The pion asymmetry for the reaction $p + p \rightarrow \pi^+ + d$. The asymmetry for the reaction $p + p \rightarrow \pi^+ + p + n$ measured in this experiment is included for comparison. If only s - and p -wave pions are emitted, the asymmetry is given by $\epsilon = \Delta P A \sin \theta / (A + \cos^2 \theta)$, where P is the beam polarization, $(A + \cos^2 \theta)$ is the angular distribution for an unpolarized beam, and Δ is the quantity plotted. The reference points listed are as follows: (a) Iu. K. Akimov, O. V. Savchenko, and L. M. Soroko, Soviet Phys.—JETP 8, 64 (1959) and Nuclear Phys. 8, 637 (1958); (b) A. M. Sachs, H. Winick, and B. A. Wooten, Phys. Rev. 109, 1733 (1958); (c) T. H. Fields, J. G. Fox, J. A. Kane, R. A. Stallwood, and R. B. Sutton, Phys. Rev. 109, 1704 (1958).

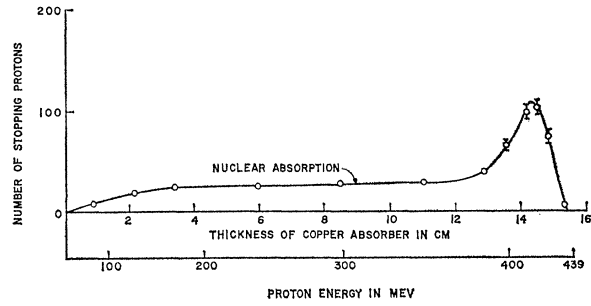


FIG. 4. Differential range curve of the polarized proton beam. The counting rate for absorber thicknesses less than 12 cm is due to nuclear absorption rather than to a low-energy component of the beam.

20% of the film was scanned twice in order to measure the scanning efficiency; it was found to be $(90 \pm 3)\%$ with no apparent systematic variations between the two scanners, or between the two sides of the beam. During the scanning, the following quantities were measured for each stopping pion: (1) the angle of the track as it entered the chamber, (2) the position of the entrance point, and (3) the position of the stopping point. The angle typically could be measured with a precision of about 0.5° . The scattered protons were counted with the aid of a template designed to exclude tracks not originating in the hydrogen. The proton count was made successively on pictures from alternate sides of the beam.

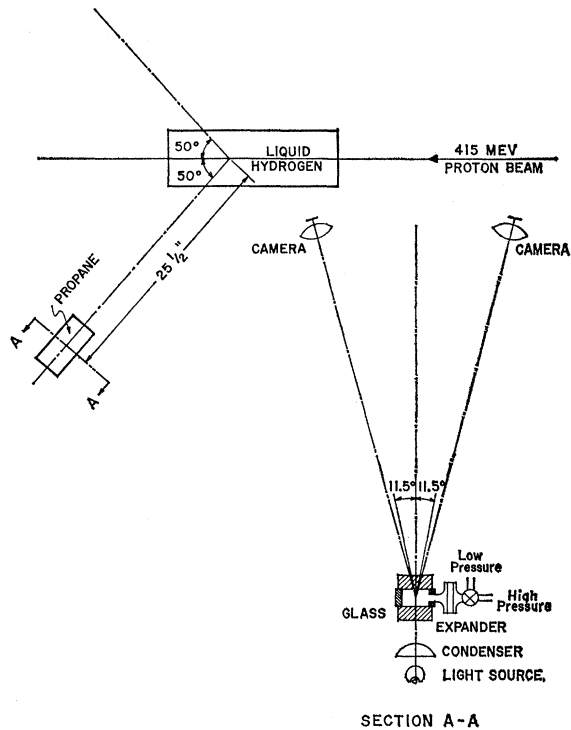


FIG. 5. Experimental arrangement.

ASYMMETRY MEASUREMENT

The pion asymmetry was defined as

$$\epsilon = (R/I_R - L/I_L) / (R/I_R + L/I_L), \quad (3)$$

where R and L are the number of pions produced to the right and left of the beam, respectively, and I_R and I_L are the integrated incident fluxes for the two cases. In terms of observed quantities, the asymmetry is

$$\epsilon = [RL_p(1+E_p) - LR_p(1-E_p)] / [RL_p(1+E_p) + LR_p(1-E_p)], \quad (4)$$

where E_p is the previously measured asymmetry in p - p scattering, and L_p and R_p are the number of scattered protons observed in the two cases.

To determine the number of pions originating in the hydrogen, it was necessary to subtract the background (pions originating in the target ends). Because of multiple scattering of the pions in the front wall of the chamber, it was not possible to separate the background unambiguously without an excessive loss of intensity. The chamber front wall was stainless steel of thickness 0.1 in. and gave a calculated projected rms multiple scattering angle of 4.5° . The procedure used to estimate the background from the target ends was as follows: Figure 6 shows the angular distribution of protons scattered from the copper "dummy" target. There are enough tracks to determine accurately the mean and the width of each peak. Since these were tracks of high-energy protons, multiple scattering made only a small contribution to the widths. The calculated multiple scattering of pions in the stainless-steel entrance window was folded into these curves to obtain the shape of the pion distribution from the target ends. The normalization of the pion background curves was obtained by making a least-squares fit to the ends of the observed pion angular distribution as shown in Fig. 7. (Figure 7 shows data which represent an average for the two sides of the beam. In the actual data reduction, the above analysis was performed separately for left and for right scattering.)

Because of the sharp angular dependence of the background, there is an optimal angular region (between

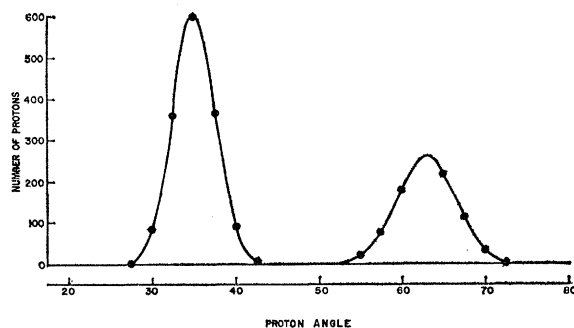


FIG. 6. Angular distribution of protons scattered from copper placed at the position of the target ends.

38 and 60°) for which the net error is a minimum. The background (from the target ends) contributes approximately 16% of the total counting rate in this region. The observed asymmetry was $\epsilon = -(19.9 \pm 6.5)\%$, based on a total of 396 pions. The sign of the asymmetry is the same as that previously observed for reaction (1). The error is mainly of statistical origin, but includes small contributions from uncertainties in the background subtraction method and from the estimated error (0.3°) in the 50° angle between the beam and chamber axis.

An independent check of the chamber orientation was made by observing the range and angle of elastically scattered protons which came to rest in the propane. This method yielded a chamber angle of $(50.1 \pm 0.4)^\circ$ on one side of the beam and $(49.9 \pm 0.4)^\circ$ on the other, affirming the direct measurement of the chamber locations to the required accuracy.

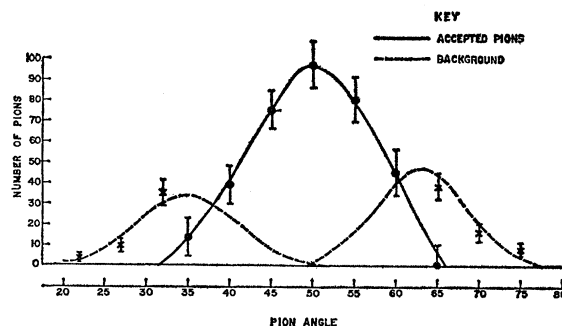


FIG. 7. The observed pion angular distribution.

CROSS-SECTION MEASUREMENT

The observed ratio of stopped pions to protons in the chamber was used to calculate an average value for the pion production differential cross section. The total number of stopping pions was 333, with a laboratory angular range of 40 – 58° and a laboratory energy range of 30 – 55 MeV. The total number of elastically scattered protons was 2.28×10^5 . The pion to proton ratio was subjected to the following corrections: azimuthal asymmetry in the pion production and proton scattering (10%), background from target ends (12%), pion decay in flight (8.5%), and scanning efficiency (10%). A corrected π/p ratio of $(1.54 \pm 0.13) \times 10^{-3}$ was obtained. Calculation of the average pion production cross section in the center-of-mass system was then carried out using the relation

$$\left(\frac{\Delta^2 \sigma}{\Delta \Omega \Delta E} \right)_{c.m.} = \frac{\pi}{P} \frac{\int d(\text{pos}) \left(\frac{d\sigma}{d\Omega} \right)_{pp} \Delta \Omega(\text{pos})}{\int d(\text{pos}) \int dE J^{-1} \Delta \Omega(\text{pos}, E)}, \quad (5)$$

where the integration extends over the region common

to target and beam, $(d\sigma/d\Omega)_{pp}$ is the p - p cross section in the laboratory system, $\Delta\Omega(\text{pos}, E)$ is the solid angle subtended at an arbitrary position in the target, by that portion of the chamber in which the pion stops, and $\Delta\Omega(\text{pos})$ is the solid angle subtended by the front face of the chamber at an arbitrary position in the target. J is the Jacobian of the transformation from the laboratory to the center-of-mass system, and is equal to the ratio of the pion c.m. momentum to the pion lab momentum. The integrals were computed numerically; the final result was

$$\langle \Delta^2\sigma/\Delta\Omega\Delta E \rangle_{\text{c.m.}} = (0.38 \pm 0.04) \times 10^{-30} \text{ cm}^2/\text{sr MeV}.$$

DISCUSSION

Asymmetry

A comparison of the measured asymmetry, $(-20 \pm 6.5)\%$, with a previously measured value of $(-20 \pm 3)\%$ for the (pp, π^+d) reaction, indicates that nucleon final states other than 3S_1 do not make a large contribution to the pion intensity at this angle and energy.

Table I lists the possible reaction channels for (pp, π^+pn) in which the pions are produced in either s or p states and the nucleons are left in either relative S or P states. Because only the pion is observed, we must integrate over all the nucleon variables if we are to determine possible interference effects. The reactions fall into six mutually orthogonal classes; i.e., interference occurs only among two or more reactions within a single class. The only reactions producing an asymmetry at 90° are the 3S_1s and 3S_1p , the 3P_0s and 3P_0p , and the 3P_2s and 3P_2p . The other reactions, if present, will have the effect of diluting the observed asymmetry, because they will contribute symmetrically to the pion intensity. Note that the reaction (pp, π^0pp) proceeds via σ_{11} , and has a cross section at 405 MeV of about $70 \mu\text{b}$.

Qualitatively, the situation is that the asymmetry may be diluted by the presence of final-state P nucleons, and a direct contribution to the asymmetry can arise from some of the (relatively small) σ_{11} amplitudes. In view of these uncertainties as well as the experimental errors, one can only estimate the P -state contribution as being $\leq 30\%$ of the cross section at this angle and energy.

Two other measured asymmetries can be compared with the present result. An experiment by deCarvalho *et al.*³ implied that the pion azimuthal asymmetry at 90° c.m. production angle was roughly equal and opposite for the (pp, π^+d) and (pp, π^+pn) reactions; this is quite inconsistent with the present result. More recently, March has measured the pion asymmetry at 420 MeV as a function of the pion energy.⁴ He found that the pion asymmetry tends to approach zero or

TABLE I. Final states for pion production. 3P_1 , etc., are nucleon-nucleon angular momentum states, and s and p are pion orbital angular momentum states. For σ_{ij} , i is the isotopic spin for the initial state and j is the isotopic spin for the nucleons in the final state.

Cross section	Final nucleon angular momentum	Angular momentum state
σ_{10}	3S_1	${}^3P_1 \rightarrow {}^3S_1s$ ${}^1S_0 \rightarrow {}^3S_1p$ ${}^1D_2 \rightarrow {}^3S_1p$
	1P_1	${}^3P_0 \rightarrow {}^1P_1$ ${}^3P_1 \rightarrow {}^1P_1p$ ${}^3P_2 \rightarrow {}^1P_1p$ ${}^3F_2 \rightarrow {}^1P_1p$
σ_{11}	1S_0	${}^3P_0 \rightarrow {}^1S_0s$
	3P_0	${}^1S_0 \rightarrow {}^3P_0s$ ${}^3P_0 \rightarrow {}^3P_0p$ ${}^3P_1 \rightarrow {}^3P_0p$
σ_{11}	3P_1	${}^3P_0 \rightarrow {}^3P_1p$ ${}^3P_1 \rightarrow {}^3P_1p$ ${}^3P_2 \rightarrow {}^3P_1p$ ${}^3F_2 \rightarrow {}^3P_1p$
	3P_2	${}^1D_2 \rightarrow {}^3P_2s$ ${}^3P_1 \rightarrow {}^3P_2p$ ${}^3P_2 \rightarrow {}^3P_2p$ ${}^3F_2 \rightarrow {}^3P_2p$ ${}^3F_3 \rightarrow {}^3P_2p$

even reverse sign for low pion energy (possibly due to the σ_{11} contribution). An approximate averaging of March's data over the energy region covered by this experiment yields $\epsilon/P \sin\theta = -(25 \pm 18)\%$, to be compared with the present result of $\epsilon/P \sin\theta = -(38 \pm 13)\%$.

Cross Section

Before comparing the measured differential cross section with the prediction of the phenomenological theory for σ_{10}'' , we first make a rough correction for the σ_{11} contribution by reducing the measured value by the fraction

$$\sigma_{11}/(\sigma_{10}'' + \sigma_{11}) = 0.07/(0.56 + 0.07) = 11\%.$$

This correction is probably an underestimate, since the angular distribution for σ_{11} is more isotropic than for σ_{10} . The experimental result then becomes

$$d^2\sigma_{10}''/d\Omega dE = (0.34 \pm 0.04) \times 10^{-30} \text{ cm}^2/\text{sr MeV},$$

which exceeds the prediction of the threshold theory by about 20% . If we use the pion energy-angle spectrum of the threshold theory to estimate total cross sections, we obtain

$$\sigma_{10}'' = (0.56 \pm 0.06) \text{ mb},$$

$$\sigma_{\pi pn} = (0.63 \pm 0.06) \text{ mb},$$

$$\sigma_{10}''/(\sigma_{10}'' + \sigma_{10}') = (38 \pm 4)\%.$$

³ H. G. deCarvalho, E. Heiberg, J. Marshall, and L. Marshall, Phys. Rev. **94**, 1796 (1954).

⁴ R. H. March, Phys. Rev. **120**, 1874 (1960).

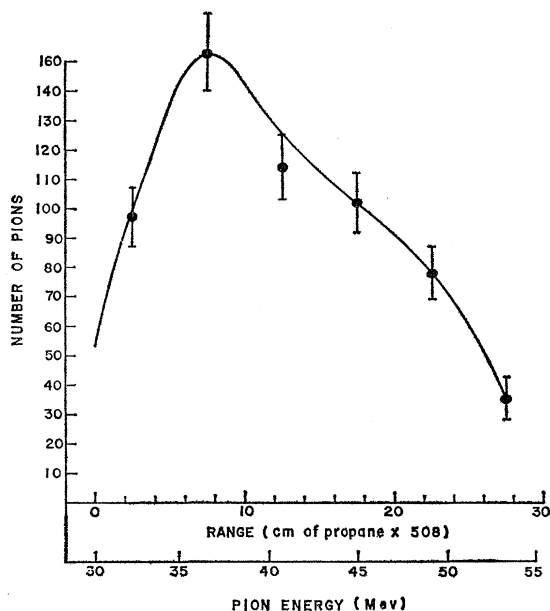


FIG. 8. Pion range distribution for all observed pions.

This value for $\sigma_{\pi pn}$ is shown on Fig. 2, and seems to be in agreement with other experimental results as well as with Mandelstam's calculation. The latter involves a $\approx 10\%$ contribution of nucleon P state to the cross section at 405 MeV, consistent with the asymmetry and cross section results of this experiment.

Figures 7 and 8 show the angle and energy distribution of the pions as observed in this experiment, where we have averaged right and left data in order to cancel polarization effects. The shapes of the curves

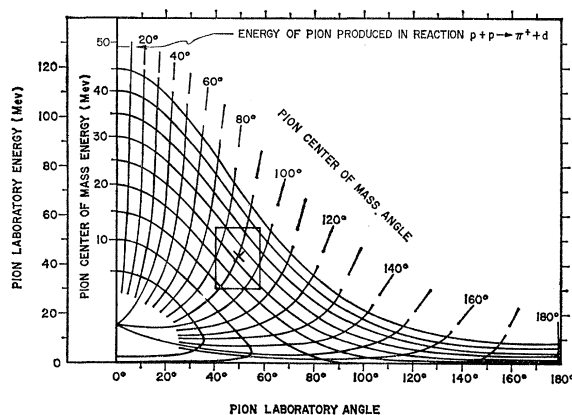


FIG. 9. Kinematical transformation between the laboratory and the center-of-mass systems. The rectangle indicates the region of observed pions.

are determined primarily by the variation of the effective solid angle with pion angle and range.

Figure 9 shows the region of angle and energy included in this experiment.

ACKNOWLEDGMENTS

The authors wish to thank Professor L. Wolfenstein and Professor R. Cutkovsky for helpful discussions of the theoretical aspects of the problem. We are grateful to E. G. Pewitt, K. Derrick, and R. Bicker for help in taking the pictures, and to the operating staff of the Nuclear Research Center for help in preparing and running the experiment. Finally, we wish to thank the scanning group and Mrs. B. Cherry for scanning the film.